OAK RIDGE NATIONAL LABORATORY
operated by
UNION CARBIDE CORPORATION
NUCLEAR DIVISION
for the
U.S. ATOMIC ENERGY COMMISSION

ORNL-TM-3242

VISCOELASTIC ANALYSIS OF IRRADIATED GRAPHITE WITH VARIABLE CREEP COEFFICIENT

S. J. Chang
J. A. Carpenter
D. W. Altom

ORNL-TM-3242

Contract No. W-7405-eng-26

Mathematics Division

VISCOELASTIC ANALYSIS OF IRRADIATED GRAPHITE WITH VARIABLE CREEP COEFFICIENT

S. J. Chang, J. A. Carpenter,
and D. W. Altom

MAY 1971

OAK RIDGE NATIONAL LABORATORY
Oak Ridge, Tennessee
operated by
UNION CARBIDE CORPORATION
for the
U. S. ATOMIC ENERGY COMMISSION

Table of Contents

Nomenclature

σ, τ	Stress
ϵ, γ	Strain
D	Accumulated neutron exposure
J_x	Creep function in the transverse plane
J_z	Creep function in the axial direction
J_{zx}	Creep function in shear
μ	Poisson's ratio
J_p	Primary creep
J_s	Secondary creep
J_o	Temperature-independent creep function
G	Relaxation function
E	Young's modulus
K	Creep coefficient
A_o	Material property constant
φ	Stress function
T_x	Boundary traction, x-component
T_y	Boundary traction, y-component
ψ	Dimensional change function
α	Coefficient of thermal expansion
T	Temperature
$T_{a,b}$	Surface temperature
Z	Coordinate in the axial direction
L	Length of the cylinder

VISCOELASTIC ANALYSIS OF IRRADIATED GRAPHITE WITH VARIABLE CREEP COEFFICIENT

S. J. Chang, J. A. Carpenter,
and D. W. Altom

ABSTRACT

This report is an addendum to a previous report[1] concerning a method of stress analysis for irradiated graphite which may be used for Molten Salt Breeder Reactor (MSBR) core design. To provide a refined analysis, the present method includes the effect of a variable creep coefficient which is caused by the nonuniform temperature distribution. To facilitate a simple formulation, it is assumed that the temperature dependence of the elastic response of the material is approximated to be inversely proportional to the creep rate. It is shown that the problem reduces to the solution of several associated (fictitious) elastic problems which have a common elastic modulus inversely proportional to the creep rate of the irradiated graphite. Numerical examples in the previous report were recalculated based on the present theory. It shows, for large dose values, an improvement to the previous method. A computer program is written for the purpose and can include the previous solution as a special case.

Keywords: stress analysis, graphite, neutron irradiation, dimensional change, temperature, viscoelasticity, lifetime, MSBR, creep coefficient.

INTRODUCTION

The graphite moderator located in a Molten Salt Breeder Reactor (MSBR) is subjected to intense neutron irradiation and temperature change. The irradiated graphite is known to exhibit the properties of creep and dimensional change which depend significantly on temperature. A report[1] was written to provide a method of stress analysis

[1] S. J. Chang, C. E. Pugh, and S. E. Moore, "Viscoelastic Analysis of Graphite Under Neutron Irradiation and Temperature Distribution," ORNL-TM-2407 (October 1969); and Fifth Southeastern Conference on Theoretical and Applied Mechanics, Raleigh, North Carolina, April 1970.

for the purpose of MSBR core design. It applied the theory of linear viscoelasticity and reduced the problem to the stress analysis of several fictitious elastic problems. It was illustrated that the method can analyze the effects of any two-dimensional geometry, boundary tractions, temperature distribution, and neutron-induced dimensional change by calculating several elastic problems.

The method, however, was based on the assumption that the creep rate K(T) was independent of temperature change throughout the cross section. This assumption, as shown in the next section, will lead to some error according to the preliminary analyses given in the previous report.[1] It is the intention of the present report to provide a modified method so that the variation of K(T) with respect to temperature is included in the formulation. The resulting analysis in the text shows that the modified formulation can also reduce the problem to the solution of several associated elastic problems. But these associated elastic problems have a common nonuniform elastic modulus, inversely proportional to K(T).

The numerical examples of the previous report were recalculated. The results show an improvement of the method of analysis. The computer program in the present case includes the previous one as a special case.

REVISED CONSTITUTIVE EQUATIONS

The purpose of this revision is to provide a reasonable concern about the variation of the creep rate K(T) with temperature in the creep function. The necessity of this modification is supported by the numerical values shown below.

The preliminary analyses for the temperature profile of the Molten Salt Breeder Reactor (MSBR) presented in a former report[1] indicated that the temperature ranges from 670°C to 760°C as shown in Fig. 4 of that report. The resulting variation in K(T), as well as its consequence in the range of large neutron dose, will provide us the obvious reason why the modified analysis in the present report is necessary. In fact, the formula shown in Eq. (55) of the earlier report shows a difference of 14% in K(T) for the temperature range from 670°C to 760°C. With a neutron dose value of $D = 3 \times 10^{22}$ nvt this will lead to a difference in creep function, shown in Eq. (19) of that report, of

$$\Delta K(T)D = 8.4 \times 10^{-6}$$

when K(T) is computed at T = 700°C. The value of $\frac{1.5}{E}$ in the creep function is 8.8×10^{-7}. $\frac{1.5}{E}$ is understood to be the sum of the instantaneous and primary creeps. Therefore, the change in $K(T) \cdot D$ in the creep function because of the temperature difference is important as compared with $\frac{1.5}{E}$. Furthermore, the term $K(T) \cdot D$ itself in the creep function for D = 3×10^{22} nvt has a higher order of magnitude as compared with $\frac{1.5}{E}$ in the creep function. These facts indicate that, in creep analyses, the variation of K(T) with temperature is not negligible and the variation of $\frac{1.5}{E}$ is of less importance. The latter fact will be used below as the approximation in our modified creep function as shown in the next paragraph. This creep function will be used later.

With the above concern, it is therefore reasonable to approximate the creep function in the following form

$$J(D) = \frac{K(T)}{K_o} J_o(D) \tag{1}$$

with

$$J_o(D) = \frac{1}{E} + \frac{1}{2E}\left(1 - e^{-A_o D}\right) + K_o \cdot D \ . \tag{2}$$

K_o is the creep coefficient K(T) computed at some average temperature and A_o is a large constant. Therefore, the initial response is represented approximately but the creep rate is exact. Hence the method is more effective for large dose range, and for temperature sensitive K(T). For lower dose range the method of the previous report[1] is more accurate. Since the present method will include the method developed previously as a special case, the solution for small dose can be obtained readily by assuming K(T) to be constant throughout the cross section in the present method. The reason that this form of approximation is proposed is that in Eq. (1), J(D) can be factored into two parts, one depending on the space coordinates, the other on dose. This factorization still can facilitate the inversion operation in a series of derivations shown in the last section of this report. The constitutive equations based on Eq. (1) for a three-dimensional body can therefore be derived similarly to that in our previous report.

With the understanding of the new form of J(D), the constitutive equations for the transversely isotropic graphites, as possessed by many kinds of graphite, are

$$\epsilon_x = J_x * (d\sigma_x - \mu_x d\sigma_y) - \mu_z J_z * d\sigma_z + \alpha_x T + \psi_x(T,D) \quad , \tag{3}$$

$$\epsilon_y = J_x * (d\sigma_y - \mu_x d\sigma_x) - \mu_z J_z * d\sigma_z + \alpha_x T + \psi_x(T,D) \quad , \tag{4}$$

$$\epsilon_z = J_z * (d\sigma_z - \mu_z d\sigma_x - \mu_z d\sigma_y) + \alpha_z T + \psi_z(T,D) \quad , \tag{5}$$

$$\gamma_{xy} = 2(1 + \mu_x)\, J_x * d\tau_{xy} \quad , \tag{6}$$

$$\gamma_{yz} = J_{zx} * d\tau_{yz} \quad , \tag{7}$$

$$\gamma_{zx} = J_{zx} * d\tau_{zx} \quad , \tag{8}$$

where z axis is assumed to be the axis of mechanical symmetry and both Poisson ratios, μ_x and μ_z, to be constant. The Poisson ratio μ_x is defined as the ratio of induced lateral strain to longitudinal strain for a uniaxial test when both directions lie in the plane of isotropy (x,y). Whereas, μ_z is the ratio of the lateral strain induced in a direction in the plane of isotropy to the longitudinal strain in the direction normal to the isotropic plane. When these ratios are dose dependent, two creep functions, in addition to J_x, J_z, and J_{zx}, are required for the stress-strain representation. The notation (*) is used to represent a convolution relation, e.g.,

$$J * d\sigma = \int_0^D J(D - D')\, \frac{\partial\sigma}{\partial D'}\, dD' \quad . \tag{9}$$

The terms αT and $\psi(T,D)$ represent the strains due to thermal expansion and dimensional changes resulting directly from neutron irradiation, respectively.

The generalized plane-strain conditions are defined by the case when the normal strain in a given direction, say the z direction, assumes a constant value ϵ_o, all derivatives with respect to z vanish, such that the net resultant force in the z direction vanishes. Under these conditions the system of equations, Eqs. (3)-(8), reduces to an equivalent two-dimensional case

$$\epsilon_x = (J_x - \mu_z^2 J_z) * d\sigma_x - (\mu_x J_x + \mu_z^2 J_z) * d\sigma_y + (\alpha_x + \mu_z \alpha_z) T + \psi_x + \mu_z \psi_z - \mu_z \epsilon_o \quad , \tag{10}$$

$$\epsilon_y = (J_x - \mu_z^2 J_z) * d\sigma_y - (\mu_x J_x + \mu_z^2 J_z) * d\sigma_x + (\alpha_x + \mu_z \alpha_z) T + \psi_x + \mu_z \psi_z - \mu_z \epsilon_o \quad , \tag{11}$$

$$\gamma_{xy} = 2(1 + \mu_x) J_x * d\tau_{xy} \quad . \tag{12}$$

For an isotropic graphite, the following simplifications can be made in the generalized plain-strain formulation:

$$\mu_z = \mu_x = \mu \quad , \tag{13}$$

$$J_x = J_z = J \quad , \tag{14}$$

$$\alpha_x = \alpha_z = \alpha \quad , \tag{15}$$

$$\psi_x = \psi_y = \psi \quad , \tag{16}$$

and it follows that

$$\epsilon_x = (1 - \mu^2)\ J * \left(d\sigma_x - \frac{\mu}{1 - \mu}\, d\sigma_y\right) + (1 + \mu)(\alpha T + \psi) - \mu\epsilon_o \ , \qquad (17)$$

$$\epsilon_y = (1 - \mu^2)\ J * \left(d\sigma_y - \frac{\mu}{1 - \mu}\, d\sigma_x\right) + (1 + \mu)(\alpha T + \psi) - \mu\epsilon_o \ , \qquad (18)$$

$$\gamma_{xy} = 2(1 + \mu)\ J * d\tau_{xy} \ . \qquad (19)$$

Thus, it is seen from Eqs. (17)-(19) that the viscoelastic stress analysis of an isotropic graphite requires the determination of only one creep function, J(D), and one Poisson ratio, μ.

FORMULATION AND SOLUTION

In this section, a method of viscoelastic stress analysis is made to correspond to several equivalent elastic problems. These fictitious elastic problems have the same moduli of elasticity, inversely proportional to the creep coefficient K(T). This differs from our previous analysis. Consider an arbitrary two-dimensional cross section where the neutron flux is assumed to be uniform over the entire section and the creep function K(T) depends on the temperature distribution. As used before,[1] the stress function, φ, is introduced by

$$\sigma_x = \frac{\partial^2\varphi}{\partial y^2} \ , \qquad (20)$$

$$\sigma_y = \frac{\partial^2\varphi}{\partial x^2} \ , \qquad (21)$$

$$\tau_{xy} = -\frac{\partial^2\varphi}{\partial x\partial y} \ , \qquad (22)$$

which will satisfy the equations of equilibrium. After substituting Eqs. (20), (21), and (22) into the equation of compatibility

$$\frac{\partial^2\epsilon_y}{\partial x^2} + \frac{\partial^2\epsilon_x}{\partial y^2} = \frac{\partial^2\gamma_{xy}}{\partial x\partial y} \ , \qquad (23)$$

the governing equation of φ is

$$J_o * d\left[\frac{\partial^2}{\partial x^2}\frac{K(T)}{K_o}\left(\frac{\partial^2\varphi}{\partial x^2} - \frac{\mu}{1-\mu}\frac{\partial^2\varphi}{\partial y^2}\right) + \frac{\partial^2}{\partial y^2}\frac{K(T)}{K_o}\left(\frac{\partial^2\varphi}{\partial y^2} - \frac{\mu}{1-\mu}\frac{\partial^2\varphi}{\partial x^2}\right) + \frac{2}{1-\mu}\frac{\partial^2}{\partial x\partial y}\frac{K(T)}{K_o}\frac{\partial^2\varphi}{\partial x\partial y}\right] = \frac{-\mu}{1-\mu}\nabla^2\left[\psi(D,T) + \alpha T\right] , \quad (24)$$

where

$$J_o = \frac{1}{E} + \frac{1}{2E}\left(1 - e^{-A_o D}\right) + K_o D . \quad (25)$$

After inversion, φ satisfies

$$\frac{\partial^2}{\partial x^2}\left[\frac{K(T)}{K_o}\left(\frac{\partial^2\varphi}{\partial x^2} - \frac{\mu}{1-\mu}\frac{\partial^2\varphi}{\partial y^2}\right)\right] + \frac{\partial^2}{\partial y^2}\left[\frac{K(T)}{K_o}\left(\frac{\partial^2\varphi}{\partial y^2} - \frac{\mu}{1-\mu}\frac{\partial^2\varphi}{\partial x^2}\right)\right] + \frac{2}{1-\mu}\frac{\partial^2}{\partial x\partial y}\left[\frac{K(T)}{K_o}\frac{\partial^2\varphi}{\partial x\partial y}\right] = \frac{-\mu}{1-\mu} G_o * d\,\nabla^2\left[\psi(D,T) + \alpha T\right] , \quad (26)$$

where G_o is related to J_o by[2]

$$\int_0^D G_o(D - D')\frac{\partial}{\partial D'} J_o(D')\,dD' = H(D) , \quad (27)$$

and $H(D)$ is the unit step function. The function G_o which corresponds to J_o given by Eq. (25) is

$$G_o(D) = \frac{E}{\sqrt{(E \cdot K_o + 1.5A_o)^2 - 4E \cdot K_o A_o}}\left[(k_1 + A_o)\,e^{k_1 D} - (k_2 + A_o)\,e^{k_2 D}\right] \quad (28)$$

where

$$k_1 = -0.5\,(E \cdot K_o + 1.5A_o) + 0.5\sqrt{(E \cdot K_o + 1.5A_o)^2 - 4E \cdot K_o \cdot A_o} \quad (29)$$

---

[2]E. H. Lee, "Viscoelastic Stress Analysis," Chap. 53, Handbook of Engineering Mechanics, edited by W. Flügge, McGraw-Hill, New York, 1962.

$$k_2 = -0.5(E \cdot K_o + 1.5A_o) - 0.5\sqrt{(E \cdot K_o + 1.5A_o)^2 - 4E \cdot K_o \cdot A_o} \quad . \tag{30}$$

Both k_1 and k_2 are seen to be negative. For prescribed boundary traction, the boundary conditions are

$$\frac{\partial\varphi}{\partial y} = \int_C T_x \, ds \tag{31}$$

and

$$\frac{\partial\varphi}{\partial x} = -\int_C T_y \, ds \quad , \tag{32}$$

where T_x and T_y are the x and y components of the boundary traction acting on the boundary, C, of the cross section of the body.

If the temperature-dependent neutron-induced dimensional change is given by[3]

$$\psi(D,T) = A_2(T)\, D^2 + A_1(T)\, D \quad , \tag{33}$$

then the right-hand side of Eq. (26) reduces to

$$\frac{-1}{1-\mu}\left\{G_o(D)\,\alpha\nabla^2 T + \nabla^2 A_2(T)\int_0^D G_o(D - D') \cdot 2D' \cdot dD' + \nabla^2 A_1(T)\int_0^D G_o(D - D')\, dD'\right\} \quad , \tag{34}$$

where the temperature distribution is assumed to be applied suddenly at D = 0 and to be kept constant for D > 0. The left-hand side of Eq. (26) is seen to be the same as that used in the elastic problem with nonuniform elastic modulus. The solution to the present problem can therefore be expressed by

[3] P. R. Kasten et al., "Graphite Behavior and Its Effects on MSBR Performance," Nuclear Engineering and Design 9(2), 157-195 (1969).

$$\varphi(x,y,D) = \varphi^a(x,y) + \varphi^b(x,y)\,\frac{G_o(D)}{G_o(0)} + \varphi^c(x,y)\,F_1(D) + \varphi^d(x,y)\cdot F_2(D)\ , \tag{35}$$

where φ^a, φ^b, φ^c, and φ^d are elastic solutions, corresponding to boundary tractions, thermal expansion, dimensional change $A_1(T)$, and dimensional change $A_2(T)$, respectively, and

$$F_1(D) = \frac{1}{G_o(0)} \int_0^D G_o(D - D')\ dD' \tag{36}$$

and

$$F_2(D) = \frac{1}{G_o(0)} \int_0^D G_o(D - D')\ 2D'\ dD'\ \ . \tag{37}$$

The proof of the statement Eq. (35) can be carried out by a similar procedure as shown previously.[1] The elastic solutions are understood to be found from a nonuniform elastic medium with the common elastic modulus, $\frac{E \cdot K_o}{K(T)}$. From this consideration, the problem of irradiated graphite of an arbitrary two-dimensional cross section can be found, provided that a computer program is available to calculate the elastic thermal stress.

The displacement for the present problem due to the dimensional change and the thermal loading is the same as that obtained from a corresponding elastic problem. This result is due to the fact that the solution is independent of the creep function $J_o(D)$.

With the present formulation, a simple correspondence is made between the viscoelastic solution and the elastic solutions. The effort to solve the problem therefore reduces to the solutions φ^a, φ^b, φ^c, and φ^d. The time-dependent solution is connected with them by $F_1(D)$ and $F_2(D)$ which can be calculated from Eq. (28).

NUMERICAL EXAMPLE

Based on the theoretical formulation of the last section, the numerical examples of the previous report were recalculated. To compare the results, the curves corresponding to Figs. 6, 7, 8, 11, and 12 of

ORNL-TM-2407 are drawn and labeled as Figs. 1, 2, 3, 4, and 5 in the present report. The temperature distributions are the same as the former ones and, therefore, will not be shown here. The material constants as well as the thermal loading are the same as shown from page 13 to page 16 of the previous report. Therefore, to avoid repetition, we shall not rewrite them here.

To solve the problem numerically, we have to solve the elastic problems with the nonuniform elastic constants. Let u_i (i = 1, 2, 3) denote the radial displacements due to the volume expansions αT, $A_1(T)$, and $A_2(T)$. We recall that α is the coefficient of the linear thermal expansion shown in Eq. (15), and $A_1(T)$ and $A_2(T)$ are given by Eq. (33) and more specifically by reference 3. The problem reduces mathematically to the solution of a second-order linear ordinary differential equation of the following form:

$$\frac{d}{dr}\left[\left(\frac{\lambda + 2\mu}{E}\right)\frac{du_i}{dr}\right] + \frac{\lambda + 2\mu}{E}\,\frac{1}{r}\,\frac{du_i}{dr} - \frac{\lambda + 2\mu}{E}\,\frac{u_i}{r^2} + \left(\epsilon_i + \frac{u_i}{r}\right)\frac{d}{dr}\left(\frac{\lambda}{E}\right) = \frac{d}{dr}\left[\frac{3\lambda + 2\mu}{E}\,F_i\right] \quad (i = 1,2,3) \qquad (38)$$

where $F_1 = \alpha T$, $F_2 = A_1(T)$, and $F_3 = A_2(T)$. In Eq. (38), ϵ_i (i = 1,2,3) correspond to the three axial strains because the problems are solved under the assumption of the generalized plane strain. λ and μ are respectively defined by

$$\frac{\lambda}{E} = \frac{\sigma}{(1+\sigma)(1 - 2\sigma)}\,\frac{K_o}{K(T)} \qquad (39)$$

and

$$\frac{\mu}{E} = \frac{1}{2(1 + \sigma)}\,\frac{K_o}{K(T)}\ , \qquad (40)$$

where K(T) is defined by Eq. (1) and K_o and E are the values of K(T) and Young's modulus when T is evaluated at the inner surface of the concentric cylinder r = a. σ is the Poisson's ratio. Since T varies along r so do λ and μ.

The two integration constants for Eq. (38) and ϵ_i are to be determined by the boundary conditions

$$\lambda \left(\frac{du_i}{dr} + \frac{u_i}{r} + \epsilon_i\right) + 2\mu \frac{du_i}{dr} - (3\lambda + 2\mu) F_i = 0 \qquad (41)$$

at r = a and r = b and by the condition that the axial resultant force is zero, that is

$$\int_a^b \lambda \left[\left(\frac{du_i}{dr} + \frac{u_i}{r}\right) - (3\lambda + 2\mu) F_i\right] rdr + \epsilon_i \int_a^b (\lambda + 2\mu)\, rdr = 0 \quad .(42)$$

The problems are solved by the method of finite differences. An iterative procedure is used to determine ϵ_i. We first assume $\epsilon_i = 0$, then u_i is calculated from Eq. (38) and the boundary conditions Eq. (41). With the known value of u_i, the first approximation of ϵ_i is calculated from Eq. (42). The process continues up to a difference of the two successive ϵ_i's smaller than 10^{-6} which is approximately equivalent to a relative error of 0.1% in the present case.

After u_i (i = 1,2,3) as well as ϵ_i (i = 1,2,3) are solved, the corresponding elastic stress components are calculated by the constitutive equations

$$\sigma_r^i = \lambda \left(\frac{du_i}{dr} + \frac{u_i}{r} + \epsilon_i\right) + 2\mu \frac{du_i}{dr} - (3\lambda + 2\mu) F_i$$

$$\sigma_\theta^i = \lambda \left(\frac{du_i}{dr} + \frac{u_i}{r} + \epsilon_i\right) + 2\mu \frac{u_i}{r} - (3\lambda + 2\mu) F_i$$

$$\sigma_z^i = \lambda \left(\frac{du_i}{dr} + \frac{u_i}{r} + \epsilon_i\right) + 2\mu\, \epsilon_i - (3\lambda + 2\mu) F_i$$

and the final dose-dependent stress components are calculated by

$$\sigma_r(D,r) = \sigma_r^1 \frac{G(D)}{E} + \sigma_r^2 F_1(D) + \sigma_r^3 F_2(D)$$

$$\sigma_\theta(D,r) = \sigma_\theta^1 \frac{G(D)}{E} + \sigma_\theta^2 F_1(D) + \sigma_\theta^3 F_2(D)$$

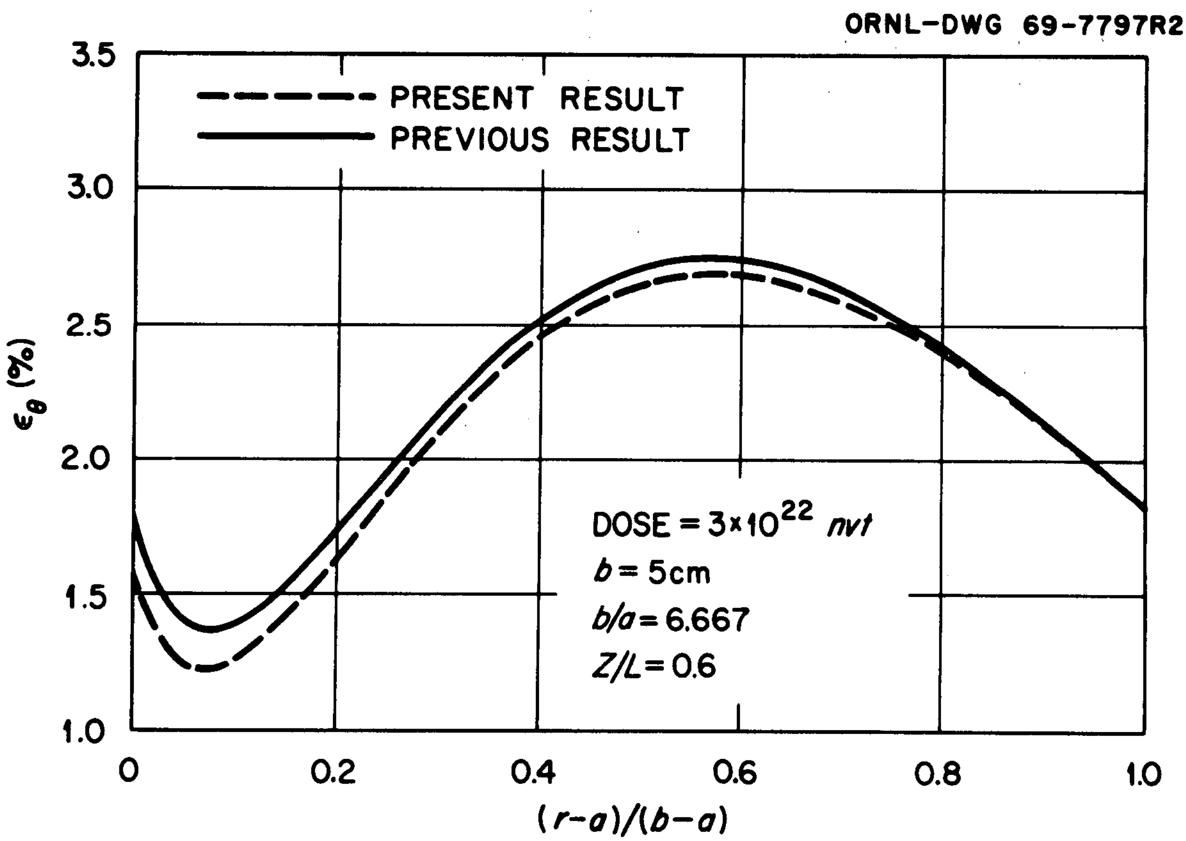

Figure 1. Circumferential Strain As a Function of Radial Position

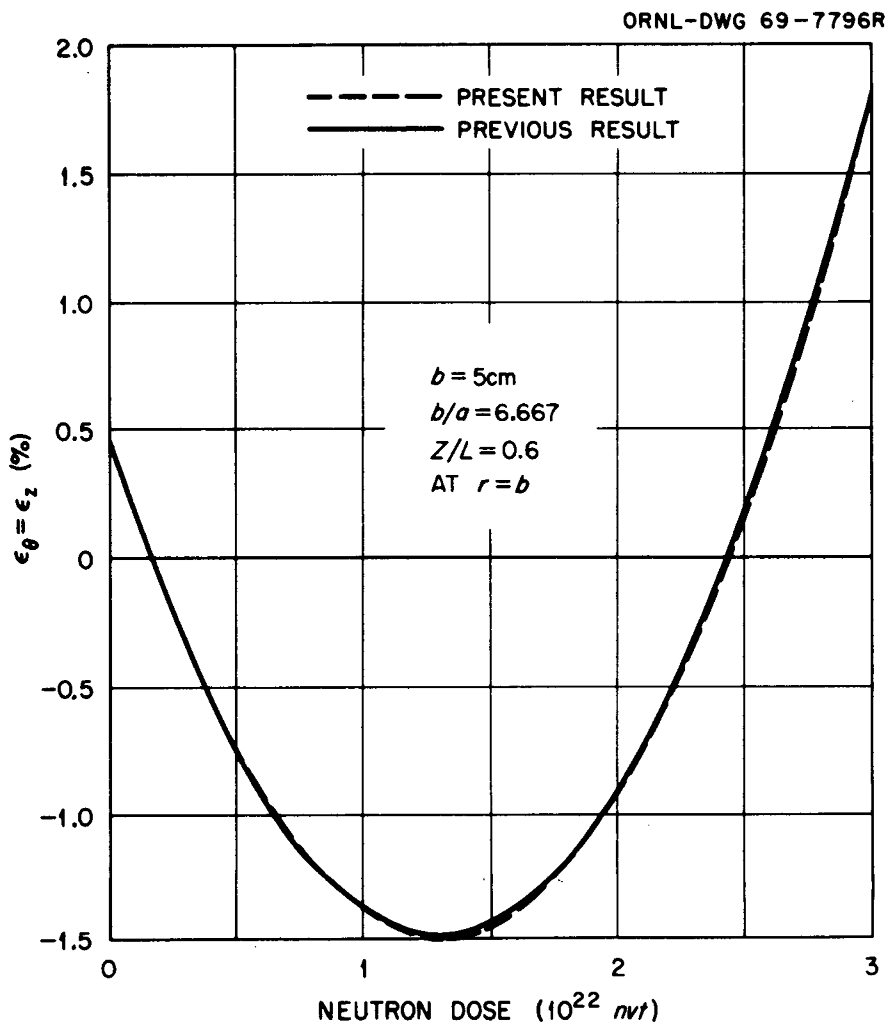

Figure 2. Circumferential Strain at Outside Surface As a Function of Fluence Level

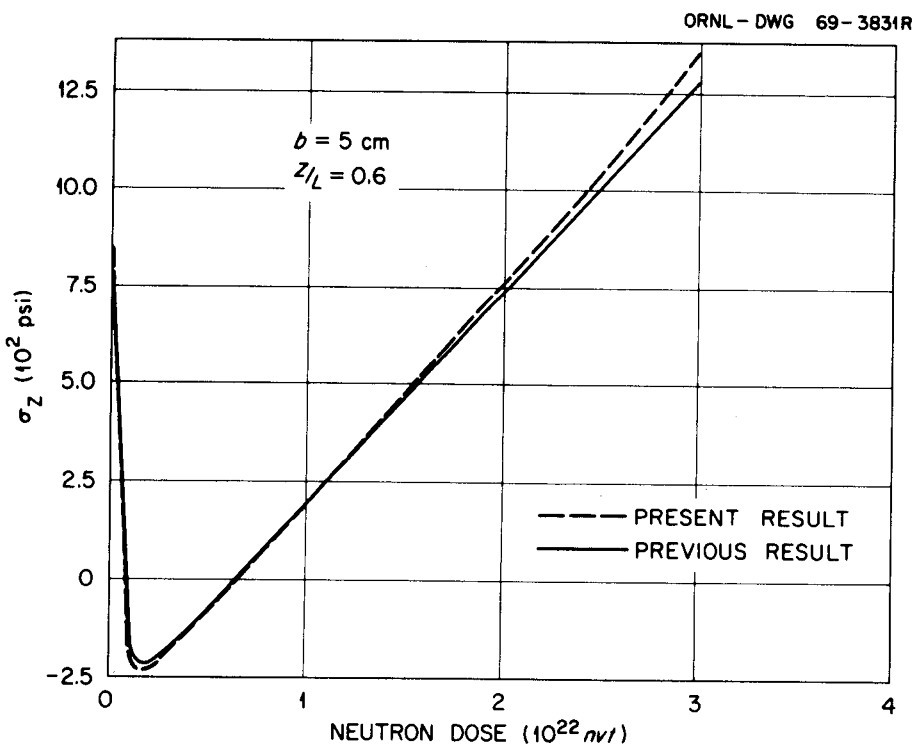

Figure 3. Axial Stress at the Outer Surface As a Function of Fluence Level

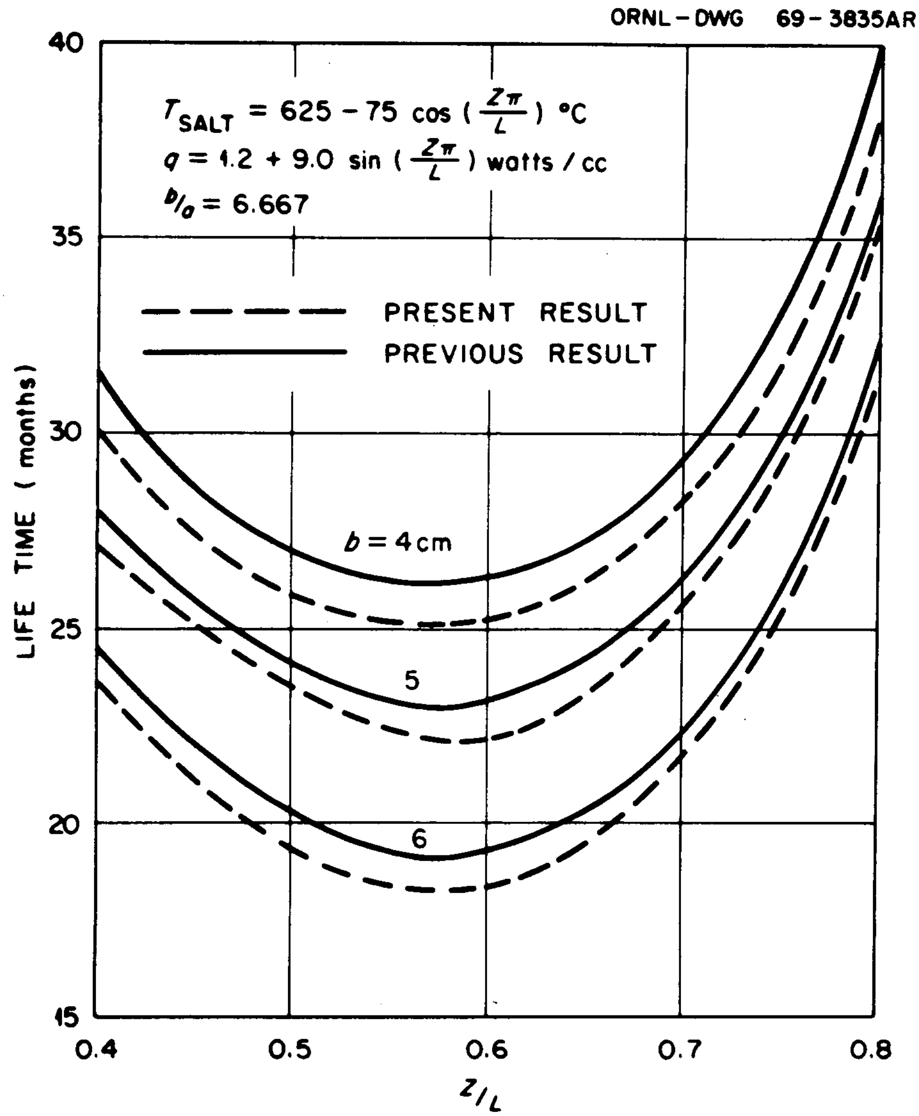

Figure 4. Lifetime of MSBR Graphite Core Cylinders As a Function of Axial Position According to the Volumetric Distortion Criterion

ORNL-DWG 69-3834A

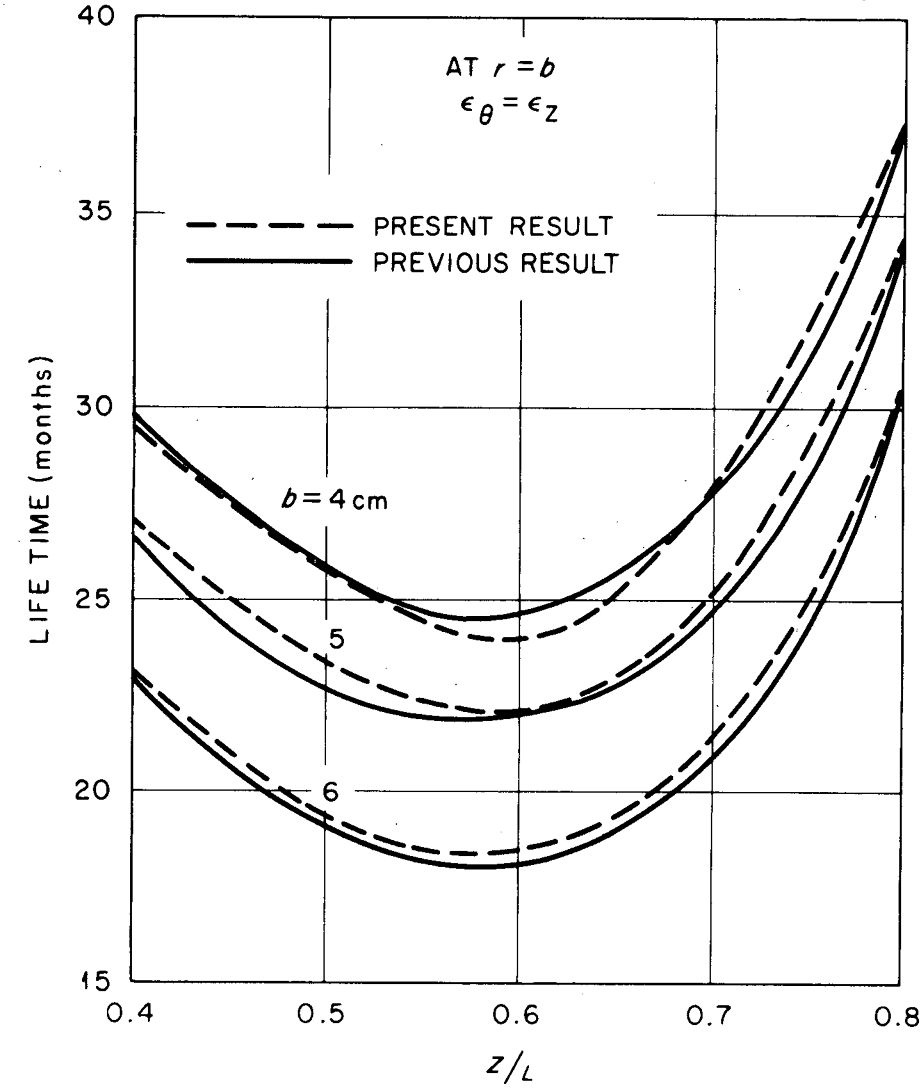

Figure 5. Lifetime of MSBR Graphite Core Cylinders As a Function of Axial Position According to the Axial Strain Criterion

$$\sigma_z(D,r) = \sigma_z^1 \frac{G(D)}{E} + \sigma_z^2 F_1(D) + \sigma^3 F_2(D) \quad .$$

The final solution of the displacement and the strain components are calculated according to

$$u = u_1 + u_2 D + u_3 D^2 \quad ,$$

$$\epsilon_r = \frac{du}{dr} \quad ,$$

$$\epsilon_\theta = \frac{u}{r} \quad ,$$

$$\epsilon_z = \epsilon_1 + \epsilon_2 D + \epsilon_3 D^2 \quad .$$

The numerical values of temperature T; displacement u; strain components ϵ_r, ϵ_θ, and ϵ_z; stress components σ_r, σ_θ, and σ_z are calculated at 41 points along the radial directions of the cylinders of b = 4,5,6 cm. The above values are calculated at each cross section of Z/L = 0.1, 0.2, ..., 0.9 for the neutron dose level D (10^{22} nvt) = 0.0, 0.2, ..., 4.0. The total computation time for an IBM 360 Model 91 machine is on the order of 4 minutes. The computing time can be reduced considerably if we reduce the error bound of ϵ_i in the iterative process.

To indicate the numerical results, typical curves are presented in Figs. 1-5 which indicate the difference from Figs. 6, 7, 8, 11, and 12 of ORNL-TM-2407. We superimposed the corresponding plots for the purpose of comparison. The reason for the difference is certainly because of a modification of J(D). The detailed explanation has been written in the paragraph following Eq. (2). The improvement is shown in Fig. 3 where σ_z at D = 3×10^{22} nvt is 13,200 psi, an increase of 6% of the previous value. This confirms our prediction.

CONCLUSION

The modified method shown in the present report has considered the effect of temperature on the creep coefficient. A difference of 6% between the components was obtained for a neutron dose level of

3×10^{22} nvt. The method is therefore important in cases when the creep coefficient is more sensitive to temperature and when the temperature gradient within the cross section is steep. The difference caused by this modification becomes more significant with increasing dose values. As the trend of the development in reactor technology is toward the higher operating temperature and the larger neutron dose level, the method presented here is therefore compatible to the need in the future. However, the instantaneous elasticity and the primary creep have an inaccurate temperature dependence imposed by the method. Therefore, the resulting solutions can be considered accurate only above some small dose value (less than $1/2 \times 10^{22}$ nvt). Below this dose value, use should be made of the previous method[1] which can be calculated by assuming a constant K(T) in the present method.

As can be seen from the derivation if the creep coefficient K(T) is taken to be constant, then the analysis will reduce to the case of our previous one. Therefore, the present computer program includes the previous one as a special case.

ACKNOWLEDGMENT

The authors express their appreciation to B. L. Greenstreet, head of the Applied Mechanics Section, for his supervision. Thanks are also due to C. E. Pugh of Applied Mechanics Section for many stimulating discussions and with whom the authors have been working for a part of the Molten Salt Breeder Reactor program.

APPENDIX

Date: 23 June 1970

Name of Program: VATCRP

Programmers: S. J. Chang, J. A. Carpenter, D. W. Altom

Description: VATCRP is a double-precision Fortran program which calculates the stress and the displacement fields for a Molten Salt Breeder Reactor graphite core under neutron irradiation and temperature distribution. VATCRP treats the creep coefficient as a function of temperature. The program is based upon the theoretical derivations and is intended to follow the proposed numerical scheme in the main text.

Three concentric cylinders are used to simulate the design study. The radius of the outer cylinder is designated B and is input to the program. The radius A of the inner cylinder is given by B/A = 6.667.

Input: The user must provide four data cards to VATCRP in the following order:

		VARIABLE NAMES	CARD FORMAT
Card 1:		BIN,DB,NB	(2D10.3,I10)
	BIN -	initial value of the radius B of the outer cylinder (in centimeters)	
	DB -	increment in the value of B (in centimeters)	
	NB -	total number of B-values, i.e., BIN ≤ B ≤ BIN + (NB-1)DB	
Card 2:		ZLIN,DZL,NZL	(2D10.3,I10)
	ZLIN -	initial value of Z/L where L is the length of the cylinders and Z is the distance measured from the bottom of the cylinders to the point of interest, i.e., 0. ≤ Z/L ≤ 1.	
	DZL -	increment in the value of Z/L	
	NZL -	total number of Z/L-values, i.e., ZLIN ≤ Z/L ≤ ZLIN + (NZL-1)DZL	

Card 3:		DIN,DD,ND	(2D10.3,I10)
	DIN -	initial value of the dose D (in 10^{22} nvt)	
	DD -	increment in the value of D	
	ND -	total number of D-values, i.e., DIN ≤ D ≤ DIN + (ND-1)DD	
Card 4:		NMAX,CRIT	(I10,D10.3)
	NMAX -	number of subintervals taken on [A,B]. NMAX nominally 40. NMAX ≤ 47.	
	CRIT -	convergence criterion of the iteration scheme outlines in the main text. CRIT nominally 10^{-6}.	

Output: Output is as described in the main text.

Language: ORNL Fortran, Fortran IV

Approximate Length:

Compiler		
ORNL	50,000	bytes
Fortran IV OPT=0	48,000	bytes
Fortran IV OPT=2	45,000	bytes

Approximate CPU Execution Timings: Data obtained using following input: BIN = 4.0, DB = 1.0, NB = 2; ZLIN = 0.1, DZL = 0.1, NZL = 2; DIN = 1.0, DD = 0.2, ND = 2; NMAX = 40, CRIT = 10^{-6}.

Compiler	360/91	360/75
ORNL	30 sec	100 sec
Fortran IV OPT=0	23 sec	78 sec
Fortran IV OPT=2	12 sec	40 sec

Computer: IBM 360 Models 75 and 91.

```
C*     *
C*     * PROGRAM VATCRP
C*     *
C      VISCOELASTIC ANALYSIS OF IRRADIATED GRAPHITE WITH VARIABLE CREEP COEF-
C      FICIENTS.  S.J.CHANG, D.W.ALTOM, J.A.CARPENTER   JUNE 1970
       IMPLICIT REAL*8(A-H,K-M,O-Z)
       COMMON/VECT/T(50),A1(50),A2(50),K(50),FF(50),LAM(50),
     1  MU(50),U(50),DURR(50)
       COMMON/SINGL/B,A,K1,K2,K1EKO,K2EKO,TT,SQP,DR,ZL,BA,EPS,DX,
     1  NMAX,NP1,NP3
       COMMCN/FOND/E1,E2,E3,E4
       DIMENSION SIGR(50,3),SIGT(50,3),SIGZ(50,3),USOL(50,3),
     1  SGR(50),SGT(50),SGZ(50),EPSR(50),EPST(50),EP(3),
     2  R(50),Z(50)
       DIMENSION F(50,3),DUDR(50,3),EPT(50)
       DATA E/1.7D6/
       DATA SIGMA/0.27D0/
       DATA ALPHA/6.2D-6/
       DATA A0/1.0D2/
       BA=6.667D0
C*     * READ INPUT PARAMETERS
       READ 1001,BIN,DB,NB
       READ 1001,ZLIN,DZL,NZL
       READ 1001,DIN,DD,ND
 1001  FORMAT(2D10.3,I10)
       READ 1002,NMAX,CRIT
 1002  FORMAT(I10,D10.3)
       NP1=NMAX+1
       NP3=NMAX+3
C*     * LOAD INITIAL OUTER RADIUS B
       B=BIN
       DO 22 I=1,NB
C*     * DETERMINE INNER RADIUS A
       A=B/BA
       RO=B-A
C*     * DETERMINE INCREMENT DR
       DR=RO/DFLOAT(NMAX)
       E1=2.0D0*DR*DR
       E2=2.0D0*DR*A
       E3=2.0D0*DR*B
       E4=DR+DR
       R(1)=A
       DO 1 N1=1,NP1
 1     R(N1+1)=R(N1)+DR
C*     * LOAD INITIAL Z/L
       ZL=ZLIN
       DO 21 J=1,NZL
C*     * CALL TMPT FOR TEMPERATURE DISTRIBUTION
       CALL TMPT
C*     * COMPUTE ARRAY CONSTANTS
       K0=(5.3D0-1.45D-2*T(2)+1.4D-5*T(2)*T(2))*1.D-5
       DO 2 I1=1,NP3
       T1=0.333333333333333D0*(0.11D0-7.0D-5*T(I1))
       T2=5.7D0-6.0D-3*T(I1)
       T3=T1/(T2*T2)
       A1(I1)=T3*2.0D0*(6.0D-3*T(I1)-5.7D0)
       A2(I1)=T3
       K(I1)=(5.3D0-1.45D-2*T(I1)+1.4D-5*T(I1)*T(I1))*1.D-5
       T1=K0/K(I1)
       LAM(I1)=(SIGMA/((1.0D0+SIGMA)*(1.0D0-SIGMA-SIGMA)))*T1
       MU(I1)=(1.0D0/(2.0D0+SIGMA+SIGMA))*T1
 2     CONTINUE
C*     * COMPUTE CONSTANTS
       TT=A0/(E*K0)
       T2=1.0D0+1.5D0*TT
       SQP=DSQRT(T2*T2-4.0D0*TT)
       K1EK0=-0.5D0*T2+0.5D0*SQP
       K2EK0=-0.5D0*T2-0.5D0*SQP
       K1=E*K0*K1EKC
       K2=E*K0*K2EK0
```

```
C*    * COMPUTE F
      DO 3 I2=1,NP3
      F(I2,1)=ALPHA*T(I2)
      F(I2,2)=A1(I2)
      F(I2,3)=A2(I2)
  3   CONTINUE
C*    *
C*    * ITERATION SCHEME
C*    *
      DO 11 II=1,3
      EPS=0.0D0
C*    * LOAD FF WITH CORRECT F ARRAY
      DO 4 J7=1,NP3
  4   FF(J7)=F(J7,II)
      IH=0
      DO 8 I4=1,10
      IH=IH+1
C*    * FINITE DIFFERENCE SCHEME
      CALL FDIFF
      DO 5 I5=1,NP1
      IT=I5+1
      Z(I5)=R(I5)*E*LAM(IT)*DURR(I5)+E*LAM(IT)*U(I5)
     1  -3.0D0*FF(IT)*R(I5)*E*LAM(IT)-2.0D0*E*MU(IT)*R(I5)*FF(IT)
  5   CONTINUE
C*    * NUMERICAL INTEGRATION
      CALL DQTFE(DR,Z,Z,NP1)
      T1=Z(NP1)
      DO 6 I6=1,NP1
      IT=I6+1
  6   Z(I6)=R(I6)*E*(LAM(IT)+2.0D0*MU(IT))
      CALL DQTFE(DR,Z,Z,NP1)
      T2=Z(NP1)
      EPN=-T1/T2
C*    * CONVERGENCE CHECK
      IF(DABS(EPS-EPN)-CRIT)9,9,7
  7   EPS=EPN
  8   CONTINUE
C*    * CONVERGENCE CRITERION MET - STORE U AND DERIVATIVES
  9   EP(II)=EPN
      DO 10 I7=1,NP1
      USOL(I7,II)=U(I7)
 10   DUDR(I7,II)=DURR(I7)
 11   CONTINUE
C*    *
      DO 13 I8=1,3
      DO 12 I9=1,NP1
      IT=I9+1
      T1=E*LAM(IT)*(DUDR(I9,I8)+USOL(I9,I8)/R(I9)+EP(I8))
      T2=E*(3.0D0*LAM(IT)+2.0D0*MU(IT))*F(IT,I8)
      T3=2.0D0*E*MU(IT)
      SIGR(I9,I8)=T1+T3*DUDR(I9,I8)-T2
      SIGT(I9,I8)=T1+T3*USOL(I9,I8)/R(I9)-T2
      SIGZ(I9,I8)=T1+T3*EP(I8)-T2
 12   CONTINUE
 13   CONTINUE
C*    * LOAD INITIAL DOSE
      D=DIN
C*    * DOSE LOOP
      DO 20 I3=1,ND
C*    * PREVENT EXPONENTIAL UNDERFLOW ON IBM 360
      IF(K2*D+170.0D0)14,14,15
 14   DX=0.0D0
      GO TO 16
 15   DX=DEXP(K2*D)
 16   T1=G(D)
      T2=F1(D)
      T3=F2(D)
      DO 17 J1=1,NP1
      SGR(J1)=SIGR(J1,1)*T1+SIGR(J1,2)*T2+SIGR(J1,3)*T3
      SGT(J1)=SIGT(J1,1)*T1+SIGT(J1,2)*T2+SIGT(J1,3)*T3
      SGZ(J1)=SIGZ(J1,1)*T1+SIGZ(J1,2)*T2+SIGZ(J1,3)*T3
```

```
 17     CONTINUE
        EPSZ=EP(1)+EP(2)*D+EP(3)*D*D
        DO 18 J2=1,NP1
        U(J2)=USOL(J2,1)+USOL(J2,2)*D+USOL(J2,3)*D*D
        EPSR(J2)=DUDR(J2,1)+DUDR(J2,2)*D+DUDR(J2,3)*D*D
        EPST(J2)=U(J2)/R(J2)
        EPT(J2)=EPSR(J2)+EPST(J2)+EPSZ
C*      * CONVERT FROM CENTIMETERS TO INCHES
        U(J2)=U(J2)/2.54DC
 18     CONTINUE
C*      *
C*      * PRINT CYCLE
C*      *
        PRINT 1003
 1003 FORMAT(1H0,36X,'B (CM)',16X,'Z/L',9X,'D (10**22 NVT)',5X,
     1  'NO. ITER.'/)
        PRINT 1004,B,ZL,D,IH
 1004 FORMAT(1H ,24X,2D20.4,D18.4,10X,I2//)
        PRINT 1005
 1005 FORMAT(1H0,2X,'(R-A)/(B-A)',3X,'TEMP DEG C',5X,'U (IN)',8X,
     1  'EPS R',5X,'EPS THETA',7X,'EPS Z',5X,'EPS TOTAL',5X,
     2  'SIGMA R',4X,'SIGMA THETA',4X,'SIGMA Z'/)
        DO 19 IK=1,NP1
        Z(IK)=(R(IK)-A)/RC
        PRINT 1006,Z(IK),T(IK+1),U(IK),EPSR(IK),EPST(IK),EPSZ,
     1    EPT(IK),SGR(IK),SGT(IK),SGZ(IK)
 1006 FORMAT(1H ,10D13.4)
 19     CONTINUE
        PRINT 1007
 1007 FORMAT(1H1)
C*      *
 20     D=D+DD
 21     ZL=ZL+DZL
 22     B=B+DB
        STOP 36264
        END


        SUBROUTINE FDIFF
CALCULATES FINITE DIFFERENCES, CALLS MATQ, AND RETURNS SOLUTION
C       VECTOR U AND DERIVATIVES OF U WITH RESPECT TC R
        IMPLICIT REAL*8(A-H,K-M,O-Z)
        COMMON/VECT/T(50),A1(50),A2(50),K(50),F(50),LAM(50),
     1  MU(50),U(50),DUDR(50)
        COMMON/SINGL/B,A,K1,K2,K1EKO,K2EKO,TT,SCP,DR,ZL,BA,EPS,DX,
     1  NMAX,NP1,NP3
        COMMCN/FOND/E1,E2,E3,E4
        DIMENSION AM(50,50)
C*      * ZERO AM
        DO 2 J=1,NP1
        DO 1 I=1,NP1
 1      AM(I,J)=C.0DO
 2      CONTINUE
C*      * FINITE DIFFERENCE EQS. AT R = A
        N=1
        G1= LAM(1)+MU(1)+MU(1)
        G2= LAM(2)+MU(2)+MU(2)
        G3= LAM(3)+MU(3)+MU(3)
        AM(1,1)=-(G3+G2+G2+G1)/E1
     1  -G2/(A*A)+(1.0D0/E2)*(LAM(3)-LAM(1))
     2  +(2.0DC*LAM(2))/G2*(DR/A)*((G2+G1)/E1
     3  -G2/E2)
        AM(1,2)=(G3+G2)/E1+G2/E2
     1  +(G2+G1)/E1-G2/E2
        U (1)=(1.0D0/E4)*((LAM(3)+LAM(3)+G3)*F(3)
     1  -( LAM(1)+LAM(1)    +G1)*F(1))
     2  +(((4.0D0*LAM(2))/G2+2.0D0)*DR*F(2)-EPS*LAM(2)*E4/G2)
     3  *((G2+G1)/E1
     4  -G2/E2)-(EPS/E4)*(LAM(3)-LAM(1))
C*      * FINITE DIFFERENCE EQS. IN ( A .LT. R .LT. B )
```

```
      NM=NMAX
      DO 3 N=2,NM
      G1= LAM(N  )+MU(N  )+MU(N  )
      G2= LAM(N+1)+MU(N+1)+MU(N+1)
      G3= LAM(N+2)+MU(N+2)+MU(N+2)
      RN=A+(N-1)*DR
      RN1=(RN+RN)*DR
      AM(N,N-1)=(G2+G1)/E1-G2/RN1
      AM(N,N)=-(G3+G2+G2+G1)/E1-G2/(RN*RN)
     1  +(LAM(N+2)-LAM(N))/RN1
      AM(N,N+1)=(G3+G2)/E1+G2/RN1
      U (N)=1.0D0/E4*((LAM(N+2)+LAM(N+2)+G3)*F(N+2)
     1  -(LAM(N)+LAM(N)+G1)*F(N))
     2  -(EPS/E4)*(LAM(N+2)-LAM(N))
    3 CONTINUE
C*    * FINITE DIFFERENCE EQS. AT R = B
      N=NP1
      G1= LAM(N    )+MU(N    )+MU(N    )
      G2= LAM(N+1  )+MU(N+1  )+MU(N+1  )
      G3= LAM(N+2  )+MU(N+2  )+MU(N+2  )
      AM(N,N-1)=(G2+G1)/E1-G2/(B*DR)
     1  +(G3+G2)/E1+G2/(B*DR)
      AM(N,N)=-(G3+G2+G2+G1)/E1
     1  -G2/(B*B)+(LAM(N+2)-LAM(N))/E3
     2  -((LAM(N+1)+LAM(N+1))/G2)*(DR/B)*((G2+G3)/E1
     3  +G2/E3)
      U (N)=1.0D0/E4*((LAM(N+2)+LAM(N+2)+G3)*F(N+2)
     1  -(LAM(N)+LAM(N)+G1)*F(N))
     2  -(((4.0D0*LAM(N+1))/G2+2.0D0)*DR*F(N+1)-EPS*LAM(N+1)*E4/G2)
     3  *((G3+G2)/E1+G2/E3)
     4  -(EPS/E4)*(LAM(N+2)-LAM(N))
C*    * SCALE
      DO 5 I=1,NP1
      U(I)=0.01D0 * U(I)
      DO 4 J=1,NP1
    4 AM(I,J)=AM(I,J) * 0.01D0
    5 CONTINUE
C*    * CALL MATQ TO OBTAIN SOLUTION VECTOR U
      CALL MATQD(AM,U,NP1,1,DET,50,50)
C*    * COMPUTE DERIVATIVES OF U WITH RESPECT TO R
      DO 6 J=2,NMAX
    6 DUDR(J)=(U(J+1)-U(J-1))/E4
      DUDR(1)=(U(2)-U(1))/DR
      DUDR(NP1)=(U(NP1)-U(NP1-1))/DR
      RETURN
      END


      SUBROUTINE TMPT
CALCULATES TEMPERATURE DISTRIBUTION
      IMPLICIT REAL*8(A-H,K-L,O-Z)
      COMMON/VECT/T(50),A1(50),A2(50),K(50),F(50),LAM(50),
     1  MU(50),U(50),DUDR(50)
      COMMON/SINGL/B,A,K1,K2,K1EK0,K2EK0,TT,SQP,DR,ZL,BA,EPS,DX,
     1  NMAX,NP1,NP3
      T1=DLOG(BA)
      T2=1.0D0-BA*BA
      TVR=(B-A)/DFLOAT(NP1-1)/A
      TSAT=625.0D0-75.0D0*DCOS(3.1415926535898D0*ZL)
      H=((1.444D-3)*TSAT-0.228D0)/A**(0.2)
      CK500=0.358D0
      SAT=TSAT
      DO 1 I=1,10
      CK=CK500*((TSAT+273.0D0)/773.0D0)**(-0.7)
      HK=H/CK
      Q=1.2D0+9.0D0*DSIN(3.141592653589 8D0*ZL)
      Q=Q*A*A/(4.0D0*CK)
      TBA=-T2/T1*Q*0.5D0*(BA+1.0D0)/B
     1  -Q*(BA+BA*BA)/B
      TBA=TBA/(HK+1.0D0/T1*(BA+1.0D0)/B)
```

```
      TAB=-T2/T1*Q*0.5D0*(BA-1.0D0)/B/HK                                TMPT 200
     1  +SAT-Q*(BA-BA*BA)/B/HK                                          TMPT 201
      TAB=TAB-TBA*(BA-1.0D0)/(B*T1*HK)                                  TMPT 210
      TA=TAB+TBA                                                        TMPT 220
      TB=TAB-TBA                                                        TMPT 230
    1 TSAT=TA                                                           TMPT 240
      CO=(TA-TB+T2*Q)/T1                                                TMPT 250
      DO 2 I=1,NP3                                                      TMPT 260
      T1=1.0D0+TVR*DFLOAT(I-2)                                          TMPT 270
      T(I)=TA-CO*DLOG(T1)-Q*(T1*T1-1.0D0)                               TMPT 280
    2 CONTINUE                                                          TMPT 290
      RETURN                                                            TMPT 300
      END                                                               TMPT 310


      DOUBLE PRECISION FUNCTION G(D)                                          10
      IMPLICIT REAL*8(A-H,K-M,O-Z)                                            20
      COMMON/SINGL/B,A,K1,K2,K1EKO,K2EKO,TT,SQP,DR,ZL,BA,EPS,DX,              30
     1  NMAX,NP1,NP3                                                          31
      G=(1.0D0/SQP)*(  (K1EKO+TT)*DEXP(K1*D)-(K2EKO+TT)*DX)                   40
      RETURN                                                                  50
      END                                                                     60


      DOUBLE PRECISION FUNCTION F1(D)                                         10
      IMPLICIT REAL*8(A-H,K-M,O-Z)                                            20
      COMMON/SINGL/B,A,K1,K2,K1EKO,K2EKO,TT,SQP,DR,ZL,BA,EPS,DX,              30
     1  NMAX,NP1,NP3                                                          31
      F1=(1.0D0/SQP)*(-(K1EKO+TT)*(1.0D0-DEXP(K1*D))/K1                       40
     1  +(K2EKO+TT)*(1.0D0-DX)/K2)                                            41
      RETURN                                                                  50
      END                                                                     60


      DOUBLE PRECISION FUNCTION F2(D)                                         10
      IMPLICIT REAL*8(A-H,K-M,O-Z)                                            20
      COMMON/SINGL/B,A,K1,K2,K1EKO,K2EKO,TT,SQP,DR,ZL,BA,EPS,DX,              30
     1  NMAX,NP1,NP3                                                          31
      F2=(2.0D0/SQP)*(-(K1EKO+TT)*(1.0D0+K1*D-DEXP(K1*D))/(K1*K1)             40
     1  +(K2EKO+TT)*(1.0D0+K2*D-DX)/(K2*K2))                                  41
      RETURN                                                                  50
      END                                                                     60

C     THIS IS ORNL D01004 OF 1167                                       DQTFE001
C     ..................................................................DQTFE002
C                                                                       DQTFE003
C        SUBROUTINE DQTFE                                               DQTFE004
C                                                                       DQTFE005
C        PURPOSE                                                        DQTFE006
C           TO COMPUTE THE VECTOR OF INTEGRAL VALUES FOR A GIVEN        DQTFE007
C           EQUIDISTANT TABLE OF FUNCTION VALUES.                       DQTFE008
C                                                                       DQTFE009
C        USAGE                                                          DQTFE010
C           CALL DQTFE (H,Y,Z,NDIM)                                     DQTFE011
C                                                                       DQTFE012
C        DESCRIPTION OF PARAMETERS                                      DQTFE013
C           H      - DOUBLE PRECISION INCREMENT OF ARGUMENT VALUES.     DQTFE014
C           Y      - DOUBLE PRECISION INPUT VECTOR OF FUNCTION VALUES.  DQTFE015
C           Z      - RESULTING DOUBLE PRECISION VECTOR OF INTEGRAL      DQTFE016
C                    VALUES. Z MAY BE IDENTICAL WITH Y.                 DQTFE017
C           NDIM   - THE DIMENSION OF VECTORS Y AND Z.                  DQTFE018
C                                                                       DQTFE019
C        REMARKS                                                        DQTFE020
C           NO ACTION IN CASE NDIM LESS THAN 1.                         DQTFE021
C                                                                       DQTFE022
C        SUBROUTINES AND FUNCTION SUBPROGRAMS REQUIRED                  DQTFE023
C           NONE                                                        DQTFE024
C                                                                       DQTFE025
```

```
C          METHOD
C             BEGINNING WITH Z(1)=0, EVALUATION OF VECTOR Z IS DONE BY
C             MEANS OF TRAPEZOIDAL RULE (SECOND ORDER FORMULA).
C             FOR REFERENCE, SEE
C             F.B.HILDEBRAND, INTRODUCTION TO NUMERICAL ANALYSIS,
C             MCGRAW-HILL, NEW YORK/TORONTO/LONDON, 1956, PP.75.
C
C     ..................................................................
C
      SUBROUTINE DQTFE(H,Y,Z,NDIM)
C
C
      DIMENSION Y(1),Z(1)
      DOUBLE PRECISION Y,Z,H,HH,SUM1,SUM2
C
      SUM2=0.D0
      IF(NDIM-1)4,3,1
    1 HH=.5D0*H
C
C     INTEGRATION LOOP
      DO 2 I=2,NDIM
      SUM1=SUM2
      SUM2=SUM2+HH*(Y(I)+Y(I-1))
    2 Z(I-1)=SUM1
    3 Z(NDIM)=SUM2
    4 RETURN
      END


C     THIS IS ORNL F04013 OF 1167
      SUBROUTINE MATQD (A,X,NR,NV,DET,NA,NX)
      IMPLICIT REAL*8(A-H,O-Z)
      DIMENSION A(961),X(31)
      DET=1.0
      NR1=NR-1
      DO 12 K=1,NR1
      IR1=K+1
      PIVOT=0.0
      DO 2 I=K,NR
      IK=(K-1)*NA+I
      Z=DABS(A(IK))
      IF(Z-PIVOT)2,2,1
    1 PIVOT=Z
      IPR=I
    2 CONTINUE
      IF(PIVOT)4,3,4
    3 DET=0.0
      RETURN
    4 IF(IPR-K)5,8,5
    5 DO 6 J=K,NR
      IPRJ=(J-1)*NA+IPR
      Z=A(IPRJ)
      KJ=(J-1)*NA+K
      A(IPRJ)=A(KJ)
    6 A(KJ)=Z
      DO 7 J=1,NV
      IPRJ=(J-1)*NX+IPR
      Z=X(IPRJ)
      KJ=(J-1)*NX+K
      X(IPRJ)=X(KJ)
    7 X(KJ)=Z
      DET=-DET
    8 KK=(K-1)*NA+K
      DET=DET*A(KK)
      DO 9 J=IR1,NR
      KJ=(J-1)*NA+K
      A(KJ)=A(KJ)/A(KK)
      DO 9 I=IR1,NR
      IJ=(J-1)*NA+I
      IK=(K-1)*NA+I
```

```
9      A(IJ)=A(IJ)-A(IK)*A(KJ)
       DO 12 J=1,NV
       KJ=(J-1)*NX+K
       IF(X(KJ)) 10,12,10
10     X(KJ)=X(KJ)/A(KK)
       DO 11 I=IR1,NR
       IJ=(J-1)*NX+I
       IK=(K-1)*NA+I
11     X(IJ)=X(IJ)-A(IK)*X(KJ)
12     CONTINUE
       NRNR=(NR-1)*NA+NR
       IF(A(NRNR)) 13,3,13
13     DET=DET*A(NRNR)
       DO 15 J=1,NV
       NRJ=(J-1)*NX+NR
       X(NRJ)=X(NRJ)/A(NRNR)
       DO 15 K=1,NR1
       I=NR-K
       SUM=0.0
       DO 14 L=I,NR1
       IL=L*NA+I
       LJ=(J-1)*NX+(L+1)
14     SUM=SUM+A(IL)*X(LJ)
       IJ=(J-1)*NX+I
15     X(IJ)=X(IJ)-SUM
       RETURN
       END
```

ORNL-TM-3242

INTERNAL DISTRIBUTION

1. R. E. Adams
2-4. D. W. Altom
5. J. L. Anderson
6. C. F. Baes
7. S. E. Beall
8. M. Bender
9. E. S. Bettis
10. D. S. Billington
11. E. G. Bohlmann
12. S. E. Bolt
13. C. J. Borkowski
14. G. E. Boyd
15. R. B. Briggs
16. A. A. Brooks
17. J. W. Bryson
18. J. P. Callahan
19. D. W. Cardwell
20-22. J. A. Carpenter
23. H. P. Carter
24-33. S. J. Chang
34. C. W. Collins
35. W. H. Cook
36. W. B. Cottrell
37. J. M. Corum
38. J. S. Crowell
39. F. L. Culler
40. R. W. Derby
41. S. J. Ditto
42. W. G. Dodge
43-45. W. P. Eatherly
46. M. Feliciano
47. D. E. Ferguson
48. L. M. Ferris
49. M. Fontana
50. A. P. Fraas
51. J. H. Frye
52. C. H. Gabbard
53-57. B. L. Greenstreet
58. W. R. Grimes
59. A. G. Grindell
60. R. C. Gwaltney
61. P. N. Haubenreich
62. D. M. Hewette, II
63. F. J. Homan
64. W. H. Jordan
65-111. P. R. Kasten
112. M. T. Kelley
113. C. R. Kennedy
114. R. B. Korsmeyer
115. K. C. Liu
116. M. I. Lundin
117. R. N. Lyon
118. R. E. MacPherson
119. W. J. McAfee
120. H. E. McCoy
121. H. C. McCurdy
122. H. A. McLain
123. L. E. McNeese
124. J. R. McWherter
125. J. G. Merkle
126. A. S. Meyer
127. A. J. Miller
128. R. L. Moore
129. S. E. Moore
130. E. L. Nicholson
131. A. M. Perry
132. J. W. Prados
133. C. E. Pugh
134. J. N. Robinson
135-136. M. W. Rosenthal
137. W. K. Sartory
138. A. W. Savolainen
139. Dunlap Scott
140. J. L. Scott
141. J. E. Smith
142. I. Spiewak
143. J. R. Tallackson
144. R. E. Thoma
145. D. B. Trauger
146. R. S. Valachovic
147. G. M. Watson
148. J. R. Weir
149. M. E. Whatley
150. J. C. White
151. G. D. Whitman
152. G. T. Yahr
153. Gale Young
154-155. Central Research Library
156. Document Reference Section
157. Laboratory Records Dept. (RC)
158-162. Laboratory Records Dept.
163. ORNL Patent Office
164. Laboratory and University Division, ORO

165-166. Division of Technical Information Extension
167-176. ORNL Mathematics Division

EXTERNAL DISTRIBUTION

177. H. W. Babel, Douglas Aircraft Co., Santa Monica, California
178. B. L. Bailey, Great Lakes Carbon Corp., Niagara Falls, New York
179. H. W. Behrman, RDT Site Office, Oak Ridge National Laboratory
180. E. O. Bergman, National Engineering Science Co., Pasadena, California
181. J. C. Bokros, Gulf General Atomic, San Diego, California
182. S. A. Bortz, IIT Research Institute, Chicago, Illinois
183. R. K. Carlson, POCO Graphite, Inc., Garland, Texas
184. W. S. Clouser, Los Alamos Scientific Laboratory, Los Alamos, New Mexico
185. H. T. Corten, University of Illinois, Urbana, Illinois
186. W. E. Crowe, Los Alamos Scientific Laboratory, Los Alamos, New Mexico
187. Jack Cully, SNPO-A, USAEC, Box 5400, Albuquerque, New Mexico
188. R. J. Dietz, Los Alamos Scientific Laboratory, Los Alamos, New Mexico
189. A. J. Edmondson, University of Tennessee, Knoxville, Tennessee
190. R. P. Felgar, TRW Systems, Redondo Beach, California
191. D. M. Forney, Air Force Materials Laboratory, Wright Patterson Air Force Base, Ohio
192. C. W. Funk, Aerojet-General Corporation, Sacramento, California
193. J. J. Gangler, National Aeronautics and Space Administration, Washington, D. C.
194. Harold Hessing, SNPO-A, Los Alamos Scientific Laboratory, CMB Division, Los Alamos, New Mexico
195. R. W. Holland, University of Tennessee, Knoxville, Tennessee
196. L. E. Hulbert, Battelle Memorial Institute, Columbus, Ohio
197. B. T. Kelley, UKAEA, Culcheth, Warrington, Lancashire, England
198. J. J. Krochmal, Air Force Materials Laboratory, Wright-Patterson Air Force Base, Ohio
199. R. G. Lawton, Los Alamos Scientific Laboratory, Los Alamos, New Mexico
200. C. W. Lee, University of Tennessee, Knoxville, Tennessee
201. J. J. Lombardo, NASA Lewis Research Center, Cleveland, Ohio
202. H. H. W. Losty, The General Electric Co., Ltd., HIRST Research Centre, Wembley, England
203. L. L. Lyon, Los Alamos Scientific Laboratory, Los Alamos, New Mexico
204. D. P. MacMillan, Los Alamos Scientific Laboratory, Los Alamos, New Mexico
205. M. Manjoine, Westinghouse Astronuclear Laboratory, Pittsburgh, Pennsylvania
206. H. E. Martens, Jet Propulsion Laboratory, Pasadena, California
207. R. L. Maxwell, University of Tennessee, Knoxville, Tennessee
208. J. T. Meers, Parma Research Center, Cleveland, Ohio
209. Captain W. E. Mercer, III, SYMSE, U. S. Air Force, Norton Air Force Base, California
210. J. L. Mershon, U. S. Atomic Energy Commission, Washington, D. C.
211. R. A. Meyer, Douglas Aircraft Co., Santa Monica, California
212. W. C. Morgan, Pacific-Northwest Laboratory, Richland, Washington
213. J. E. Morrissey, SNPO, U. S. Atomic Energy Commission, Washington, D. C.
214. R. E. Nightingale, Pacific-Northwest Laboratory, Richland, Washington
215. E. T. Onat, Yale University, New Haven, Connecticut
216. C. D. Pears, Southern Research Institute, Birmingham, Alabama

217. Hui Pih, University of Tennessee, Knoxville, Tennessee
218. D. L. Platus, Mechanics Research, Inc., El Segundo, California
219. C. A. Pratt, Air Force Materials Laboratory, Wright-Patterson Air Force Base, Ohio
220. W. G. Ramke, Air Force Materials Laboratory, Wright-Patterson Air Force Base, Ohio
221. J. C. Rowley, Los Alamos Scientific Laboratory, Los Alamos, New Mexico
222. W. S. Scheib, SNPO, U. S. Atomic Energy Commission, Washington, D. C.
223. R. W. Schneider, Bonney Forge, Allentown, Pennsylvania
224. F. C. Schwenk, SNPO, U. S. Atomic Energy Commission, Washington, D. C.
225. E. J. Seldin, Parma Research Center, Cleveland, Ohio
226. W. A. Shaw, Auburn University, Auburn, Alabama
227. L. R. Shobe, University of Tennessee, Knoxville, Tennessee
228. R. H. Singleton, Westinghouse Astronuclear Laboratory, Pittsburgh, Pennsylvania
229. C. V. L. Smith, U. S. Atomic Energy Commission, Washington, D. C.
230. M. C. Smith, Los Alamos Scientific Laboratory, Los Alamos, New Mexico
231. G. B. Spence, Parma Research Center, Cleveland, Ohio
232. W. F. Swinson, Auburn University, Auburn, Alabama
233. Norman R. Thielke, SNPO, NASA Lewis Research Center, Cleveland, Ohio
234. Ru-Lung Weng, Parma Research Center, Cleveland, Ohio